UDC 620.179.147:519.853.6 https://doi.org/10.20998/2074-272X.2025.1.01

V.Ya. Halchenko, R.V. Trembovetska, V.V. Tychkov

Computer-economical optimization method for solving inverse problems of determining electrophysical properties of objects in eddy current structroscopy

Introduction. *The problems of determining the profiles of electrophysical material properties are among the inverse problems of electrodynamics. In these studies, the focus is on the creation of a computer-economical method for reconstructing the profiles of electrical conductivity and magnetic permeability of metal planar objects under testing. These parameters can include the information about the results and quality of the production process or the effects of exposure to an aggressive environment. Registration of changes in electrophysical properties by means of eddy current testing allows for prompt adoption of effective management decisions regarding controlled processes. The simultaneous determination of these parameters because of non-contact indirect measurements of the electromotive force (EMF) by surface eddy current probes over the surface object with the subsequent restoration of the parameter distributions along its thickness by numerical methods is an urgent task.* ***Objective.*** *To create a computer-economical method for determining the electrophysical properties of objects by means of surrogate optimization with the accumulation of additional apriori knowledge about them in neural network metamodels with nonlinearly reduced dimensionality to improve the accuracy of simultaneous profile determination.* ***Methodology.*** *The method for determining the electrophysical properties of objects is based on homogeneous designs of experiments, surrogate optimization with the accumulation of apriori knowledge about them in metamodels with nonlinearly reduced dimensionality.* ***Originality.*** *Integration of multiple capabilities in the surrogate model that combine the advantages of high-performance computing and optimization algorithms in the factor space reduced by the Kernel PCA (Principal Component Analysis) method. The accumulated additional apriori knowledge about objects is incorporated into the neural network metamodel. This makes it possible to implicitly identify complex patterns hidden in the data that are characteristic of the eddy current measuring process and take them into account during reconstruction.* ***Results.*** *The reduction of the search space is a considerable result. It was possible due to the nonlinear Kernel-PCA transformations with the analysis of the eigenvalues of the kernel matrix and the restriction on the number of PCA principal components. The results confirmed the validity of a significant reduction in space without major loss of information. Another indicator of the effectiveness of the method is a high precision of the created surrogate models. The accuracy of the reduced dimensional metamodels was achieved by using a homogeneous computer design of experiment and deep learning networks. The adequacy and informativeness of the constructed surrogate models have been proved by numerical indicators. The efficiency of the method is demonstrated on model examples.* References 36, table 5, figures 6.

Key words: **inverse problems, optimization method, eddy current measurings, reconstruction, material electrophysical properties, surrogate neural network models of reduced dimensionality, apriori information, global extremum.**

Вступ. *Серед обернених задач електродинаміки певну частину складають задачі визначення профілів електрофізичних властивостей матеріалів. В цих дослідженнях акцентується увага на створенні обчислювально-економного методу реконструкції профілів електричної провідності та магнітної проникності металевих пласких об'єктів контролю. Ці параметри можуть нести інформацію щодо результатів та якості виробничого процесу або наслідків впливу на об'єкт агресивного середовища. Реєстрація змін електрофізичних властивостей засобами вихрострумового контролю дозволяє здійснювати оперативне прийняття ефективних управлінських рішень щодо контрольованих процесів. Одночасне визначення вказаних параметрів у результаті безконтактних непрямих вимірювань електрорушійної сили (ЕРС) накладними вихрострумовими перетворювачами над поверхнею об'єкту із наступним відновленням розподілів параметрів вздовж його товщі чисельними методами є актуальним завданням.* ***Мета.*** *Створення обчислювально-економного методу визначення електрофізичних властивостей об'єктів засобами сурогатної оптимізації із накопиченням додаткових апріорних знань щодо них у нейромережевих метамоделях із нелінійно-скороченою розмірністю для підвищення точності одночасного визначення профілів.* ***Методологія.*** *Метод визначення електрофізичних властивостей об'єктів створюється на основі однорідних планів експериментів, сурогатної оптимізації із накопиченням апріорних знань щодо них у метамоделях із нелінійно-скороченою розмірністю.* ***Оригінальність.*** *Інтеграція у сурогатній моделі комбінованих можливостей, які поєднують одночасно переваги високопродуктивних обчислень та виконання оптимізаційних алгоритмів у скороченому за допомогою методу Kernel PCA-просторі факторів. Виконано інкорпорацію акумульованих додаткових апріорних знань щодо об'єктів у нейромережеву метамодель. Це дозволяє неявно визначати складні приховані в даних закономірності, котрі характерні для процесу вихрострумових вимірювань, та врахувати їх під час реконструкції.* ***Результати.*** *Суттєвим результатом є скорочення простору пошуку. Це вдалося завдяки нелінійним перетворенням Kernel-PCA з аналізом власних значень ядерної матриці і обмеженням на кількість головних компонент PCA. Отримані результати підтвердили обґрунтованість істотного скорочення простору без суттєвої втрати інформації. Іншим показником ефективності методу є висока точність створених сурогатних моделей. Точності метамоделей скороченої розмірності вдалося досягти використанням однорідного комп'ютерного плану експерименту та мереж глибокого навчання. Числовими показниками доведені адекватність та інформативність побудованих сурогатних моделей. На модельних прикладах продемонстрована ефективність методу.* Бібл. 36, табл. 5, рис. 6.

Ключові слова: **обернені задачі, оптимізаційний метод, вихрострумові вимірювання, реконструкція, електрофізичні властивості матеріалу, сурогатні нейромережеві моделі скороченої розмірності, апріорна інформація, глобальний екстремум.**

Introduction. The inverse problems of determining the material electrophysical properties of metal planar testing objects (TO) make up a rather certain part among the varieties of computational electromagnetism problems [1–3]. This is due to their considerable practical importance for industry, where they help solve different problems related to production and technology. In particular, these studies focus on the tasks of inverse identification of the electrophysical properties of metal planar test objects (TO). The typical parameters to be measured indirectly are usually the electrical conductivity (EC) and magnetic permeability (MP). In many cases, they can provide information on the results and quality of the production process or the effects of exposure to aggressive environments on the TO. Registration of changes in the electrophysical properties of the TO by means of eddy current nondestructive testing allows for the prompt adoption of effective management decisions regarding controlled processes. Therefore, the

simultaneous determination of these parameters as a result of noncontact measurements of the electromotive force (EMF) by surface eddy current probes (ECP) over the surface of the TO with the subsequent reconstruction of the distributions of EC and MP (i.e., parameter profiles) along its thickness by numerical methods is an urgent task that needs to be solved.

The problem is not trivial, since it belongs to the mathematically incorrectly posed ones [4], which are characterized by instability of the solution in the presence of noise and uncontrolled variations of the complex-valued signal generated by the ECP. The peculiarity of determining the profiles of the EC and MP is the combination of measurement procedures and numerical solution of the inverse problem on the space of the set of complex numbers, each of which introduces a corresponding specificity into their overall interaction. Although some attempts to solve this problem have been made, as, for example, in [5], they are not yet sufficiently perfect and require further progress, including on the basis of intelligent technologies.

The analysis of scientific publications on this topic shows a deep interest in this issue.

A fairly thorough analytical review of current research on the problem under consideration was made by the authors in publication [6], where they reviewed publications [7–16]. It summarizes the latest trends in the development of approaches to determining the profiles of electrophysical properties of TO materials and their inherent shortcomings. In particular, we considered optimization and data-driven methods [17] that use the achievements of artificial intelligence techniques, measurements at many fixed and swept-frequencies.

This group of papers also includes the article [13], which proposes a method of inverse identification for the experimental characterization of elastic-plastic contact in indentation problems. The second group of publications consists of studies [14–17], which differ from the achievements of the previous one by the general concept of building reverse identification procedures, which constitutes a certain alternative to the identification methods from the first group.

Thus, there is a clear trend towards the widespread use of optimization and machine learning-based methods.

When using optimization methods, researchers are focused on solving inverse problems by means of gradient-free metaheuristic algorithms for finding a global extremum, in particular Simulated Annealing, Harmony Search, Genetic Algorithms (GA), Particle Swarm Optimization (PSO), etc. and their hybrids, which minimize each other's weaknesses and add to the development of their respective strengths, ensuring efficient organization of research coverage of the multidimensional search space. In addition, it is proposed to replace resource-intensive target functions with their high-performance surrogate models, which guarantee fast and reliable computations when they are repeatedly executed. It should also be noted that the method is quite dependent on the dimensionality of the search space, i.e., the number of variables searched. This is due to the effect of the «curse of dimensionality» and requires additional special actions to reduce the dimensionality of the space.

Machine learning-based methods have their advantages and disadvantages. They are more flexible, provide better generalization capability even for data that was not used during training, and have a greater potential for processing complex data with significantly nonlinear dependencies. These methods are robust to noise and random variations in data during measurements, which has a positive impact on their reliability. Researchers consider various approaches to the implementation of intelligent technologies, including deep-learning algorithms of neural networks (artificial neural network – ANN), transfer learning, various types of ANNs from physics-informed neural networks (PINN) to generative ones, in particular variational autoencoders (VAE). However, machine learning methods often require a significant amount of data for their implementation.

To summarize, it is worth noting that hybrid optimization strategies that integrate all the advantages of the analyzed methods, should be used for further research. Thus, it is promising to use surrogate optimization with the use of proxy models (metamodels, i.e., surrogate models) of reduced dimensionality to determine the profiles of electrophysical properties of TO materials, provided that they are created on the basis of deep fully connected neural networks. Furthermore, when analyzing existing studies, the authors did not find any known approaches to incorporating additional redundant knowledge about TO into neural network metamodels, which would be useful to be included directly in them. This makes it possible to implicitly establish complex nonlinear patterns of signal formation hidden in the data during experimental measurements of the ECP, to expect a more clear reflection of the physics of the eddy current testing process by the metamodel and, accordingly, a higher identification accuracy, since the degree of transparency increases with the availability of apriori information.

The feasibility of the approach to solving the problem proposed by the authors has already been proven by their previous research [6], where they compared the results of the corresponding calculations by the classical method of surrogate optimization and an alternative method using surrogate models of reduced dimensionality. However, this reduction was carried out by linear PCA (Principal Component Analysis) transformations, which led to a reduction in the dimensionality of the metamodels by almost half. However, the use of nonlinear Kernel PCA-transformations for this purpose allows us to hope for even more convincing results.

Thus, the **aim of the paper** is to develop a computationally efficient method for determining the electrophysical properties of planar metal objects by means of surrogate optimization with the accumulation of additional apriori knowledge about them in neural network metamodels with a nonlinearly reduced dimensionality to improve the accuracy of simultaneous determination of electrical conductivity and magnetic permeability profiles in eddy current measurements when establishing their microstructural features.

Research methodology. The reconstruction of the profiles of ECs and MPs is performed by an experimental and numerical method, the sequence of stages of which

largely coincides with those proposed in [1], but with certain changes concerning the accumulation of a priori information in the neural network metamodel.

The first stage involves a single measurement with an surface ECP over a planar metal TO with the registration of a sinusoidal EMF signal e_{mes}, mathematically represented by a complex number in the exponential form of recording, i.e., with the fixation of its amplitude and phase. This completes the experimental part of the method, and all subsequent stages relate exclusively to its numerical implementation.

At the next stage, the key basic and additional parameters of the electrodynamic model that describes the measurement process and reflects the result of the interaction of the electromagnetic field with the conductive medium of the TO are determined. Hence, the main ones are the discretized profiles of the EC $\sigma_i(z)$ and MP $\mu_i(z)$, $i = 1, ..., L$, where L is the number of conditional layers of the breakdown of the zone of penetration of the electromagnetic field into the TO; and additional useful ones are the frequency f of excitation of the sensing electromagnetic field and the diameter $2 \cdot r$ of the pick-up coil of the ECP; while the lift-off distance is an additional interference. It is possible to enter all these parameters into the metamodel. The a priori information, which is also accumulated in the metamodel, also includes the laws of distribution of EC and MP. At this stage, a computerized uniform design of experiment (DOE) is also created with the mandatory input of the main model parameters, but the incorporation of certain additional parameters may take place depending on the requirements for calculation accuracy. Their addition increases the time and computing resources required to form a training sample at the points of the generated design. The accuracy of the approximation of the multidimensional nonlinear response hypersurface by the neural network metamodel depends on the properties of the design. Therefore, the design should have high homogeneity rates both in the entire search space and especially in two-dimensional projections. The organization of a detailed study of the response surface topography depends on the rational arrangement of the design points [18]. Since it is not possible to visualize the topography of the response hypersurface, it is advisable to have a uniform arrangement of points in the search space. The design is based on modified LP_τ-quasi-Sobol's sequences, the advantages and features of which are described in detail in the authors' publications [6, 19], which illustrate the method of its creation in a unit hyperspace, which provides low weighted symmetrized centered discrepancy (WSCD). After scaling to the specified dimensions of the design space, the design can be used for modeling.

At the third stage, a high-cost electrodynamic model of the eddy current testing process is used to generate a training sample and to calculate the model value of the EMF e_{mod} of the probe at the design points.

So, here we will use the solution of the corresponding forward problem of field theory, the geometric model of which is shown in Fig. 1.

A cylindrical ECP excitation coil is placed above the magnetic and conductive half-space associated with the TO. It has a rectangular cross-section of finite dimensions. The electromagnetic field is excited by a sinusoidal current I, which varies with an angular frequency $\omega = 2 \cdot \pi \cdot f$. The field is quasi-stationary, i.e., wave processes in the air are neglected. The bias currents in the TO are ignored due to their negligible values compared to the conduction currents. The excitation coil is characterized by a homogeneous current density across the cross-section i_0 and has a number of turns W. The TO is considered to be conditionally multilayer, which makes it possible to simplify the representation of continuous distributions $\sigma(z)$ and $\mu(z)$ by their piecewise constant approximation analogs of L discrete samples. The laws of distribution of the electrophysical properties of the TO are assumed to be known and determined experimentally [21]. The mathematical model was created under the assumptions of linearity, isotropy, and homogeneity of the environment. For further studies, due to its versatility and ease of use for any number of conditional layers, we chose the most popular analytical electrodynamic model Uzal-Cheng-Dodd-Deeds [21–24] in the matrix formulation in the modified Theodoulidis form [25].

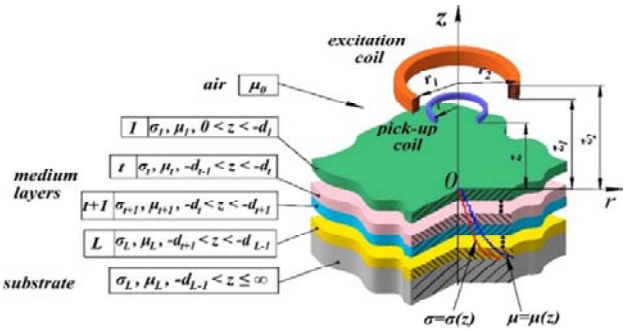

Fig. 1. Geometric model of the forward problem [20]

The magnetic vector potential in the lift-off below the ECP excitation coil is formed by summing its two components, namely, the primary potential $A^{(s)}$ of the coil itself in free space without the presence of the TO and the secondary potential $A^{(ec)}$ created by eddy currents induced in the object:

$$A_0 = A^{(s)} + A^{(ec)}. \quad (1)$$

The primary field of the excitation coil is calculated according to the expression:

$$A^{(s)} \int_0^\infty J_1(\kappa r) \cdot C_s \cdot e^{\kappa z} \kappa r, \quad (2)$$

where

$$C_s = \frac{\mu_0 \cdot i_0}{2} \cdot \frac{\chi(\kappa r_1, \kappa r_2)}{\kappa^3} \cdot \left(e^{-\kappa z_1} - e^{-\kappa z_2}\right),$$

$$\chi(x_1, x_2) = \left\{ x_1 \cdot J_0(x_1) - 2 \cdot \sum_{m=0}^{\infty} J_{2m+1}(x_1) \right\} -$$

$$- \left\{ x_2 \cdot J_0(x_2) - 2 \cdot \sum_{m=0}^{\infty} J_{2m+1}(x_2) \right\},$$

$i_0 = W \cdot I \cdot (r_2 - r_1)^{-1} \cdot (z_2 - z_1)^{-1}$, $\mu_0 = 4 \cdot \pi \cdot 10^{-7}$ H/m is a magnetic constant.

The secondary field is calculated according to the solution of the boundary value problem in the form of a second-order partial differential equation for the

azimuthal component of the magnetic vector potential A in the cylindrical coordinate system, which is valid for axially symmetric systems:

$$A\frac{\partial^2 A}{\partial r^2}+\frac{1}{r}\cdot\frac{\partial A}{\partial r}-\frac{A}{r^2}+\frac{\partial^2 A}{\partial z^2}=k^2\cdot A\,, \qquad (3)$$

where $k^2=j\cdot\omega\cdot\mu_r\cdot\mu_0\cdot\sigma$, $j=\sqrt{-1}$; under the given boundary conditions

$$\left[\begin{array}{c} A_0=A_1 \\ \dfrac{\partial A_0}{\partial z}=\dfrac{1}{\mu_{r1}}\cdot\dfrac{\partial A_1}{\partial z}\end{array}\right]_{z=0} \text{ and } \left[\begin{array}{c} A_{t+1}=A_t \\ \dfrac{1}{\mu_{t+1}}\cdot\dfrac{\partial A_{t+1}}{\partial z}=\dfrac{1}{\mu_t}\cdot\dfrac{\partial A_t}{\partial z}\end{array}\right]_{z=-d_t}. \qquad (4)$$

The solution of the boundary value problem is represented by the following expression for an arbitrary number of conditional layers of the TO:

$$A^{(ec)}\int_0^\infty J_1(\kappa r)\cdot D_{ec}\cdot e^{-\kappa z}\mathrm{d}\kappa\,, \qquad (5)$$

$$\boldsymbol{V}=\boldsymbol{T}(1,2)\cdot\boldsymbol{T}(2,3)\ldots\boldsymbol{T}(L-2,L-1)\cdot\boldsymbol{T}(L-1,L);$$

$$T_{11}(t,t+1)=\frac{1}{2}\cdot e^{(-\lambda_{t+1}+\lambda_t)dt}\cdot\left(1+\frac{\mu_t}{\mu_{t+1}}\cdot\frac{\lambda_{t+1}}{\lambda_t}\right),$$

$$D_{ec}=\frac{(\kappa\cdot\mu_{t+1}-\lambda_1)\cdot V_{11}(1)+(\kappa\cdot\mu_{t+1}+\lambda_1)\cdot V_{21}(1)}{(\kappa\cdot\mu_{t+1}+\lambda_1)\cdot V_{11}(1)+(\kappa\cdot\mu_{t+1}-\lambda_1)\cdot V_{21}(1)}\cdot C_s,$$

$$T_{12}(t,t+1)=\frac{1}{2}\cdot e^{(\lambda_{t+1}+\lambda_t)dt}\cdot\left(1-\frac{\mu_t}{\mu_{t+1}}\cdot\frac{\lambda_{t+1}}{\lambda_t}\right),$$

$$T_{21}(t,t+1)=\frac{1}{2}\cdot e^{(-\lambda_{t+1}-\lambda_t)dt}\cdot\left(1-\frac{\mu_t}{\mu_{t+1}}\cdot\frac{\lambda_{t+1}}{\lambda_t}\right),$$

$$T_{22}(t,t+1)=\frac{1}{2}\cdot e^{(\lambda_{t+1}-\lambda_t)dt}\cdot\left(1+\frac{\mu_t}{\mu_{t+1}}\cdot\frac{\lambda_{t+1}}{\lambda_t}\right),$$

$$\lambda_t=\left(\kappa^2+j\cdot\omega\cdot\mu_0\cdot\mu_t\cdot\sigma_t\right)^{1/2},$$

where $\boldsymbol{V}$ is a matrix with elements V_{11}, V_{21}; $\boldsymbol{T}()$ is a matrix with elements $T_{11}()$, $T_{12}()$, $T_{21}()$, $T_{22}()$; $J_0()$, $J_1()$, $J_m()$ are cylindrical Bessel functions of the first kind of zero, first, and m-th orders; (r_2-r_1) is the width of the cross-section of the ECP excitation coil, m; (z_2-z_1) is the height of the cross-section of the ECP excitation coil, m.

Thus, the output signal of the surface ECP induced in the pick-up coil can be calculated according to the formula:

$$e_{mod}=-j\cdot\omega\cdot w_{mes}\cdot\left[\int_{Lc}A_0(P)dl\right]_p, \qquad (6)$$

where w_{mes} is the number of turns of the pick-up coil; P is the observation point with coordinates (r, z) belonging to the contour L_c of the pick-up coil.

Thus, we finally obtain the EMF induced in the pick-up coil of the probe with a radius r:

$$e_{mod}=-j\cdot 2\cdot\pi\cdot r\cdot\omega\cdot w_{mes}\cdot A_0(P)\,. \qquad (7)$$

The verification of calculations based on the «exact» model was performed in the works of the authors [20, 26], where the results of calculations using the created software in the cases of two- and three-layer conditional representation of the TO were compared with numerical calculations by the finite element method and analytical expressions obtained for these simple idealizations. In addition, the verification was carried out by comparing the results of experimental studies conducted in [27], which recorded a sufficient level of accuracy.

The next step of the framework is to reduce the dimensionality of the search space. The purpose of these transformations is to simplify the architecture of the neural network surrogate model while simplifying it's training and increasing computational capacity and improving the conditions for the optimization algorithm. The reduction is performed by the Kernel PCA method [28, 29] with standard nonlinear transformations using the Gaussian kernel function. First, the data from the DOE are projected into a space of much higher dimensionality to obtain a kernel matrix, where linearly inseparable in the original space, significantly nonlinear data have much greater opportunities to determine independent variables with little loss of information due to the use of linear PCA. This ensures the transition to a significantly reduced dimensional PCA space with its characteristic advantages.

The fifth step is to create a neural network surrogate model. This is necessary because solving the inverse problem using an optimization implementation requires a computational model of the target function that can be used repeatedly with different parameter profiles. In this sense, model (7) creates a bottleneck in optimization, since the calculation of the non-proprietary integral of the first kind, integrals of special functions, and cumbersome combinations of special functions require quite significant expenditures of machine resources. On the other hand, a neural network metamodel also allows accumulating apriori information about the TO in advance. The metamodel is created using deep ANN techniques. The peculiarities of this stage include the need to use a CVNN (complex-valued neural network). However, in these studies, we used SCVNN (splitable complex-valued neural networks) instead of CVNN, i.e., a network split into two classical real-valued networks. They were constructed separately for the real and imaginary parts of the ECP output signal, and not for its amplitude and phase, which is essential, with subsequent combination into a common complex output. At the same time, the ANN inputs were really significant and subject to scaling. It is important for this stage to verify the adequacy and informativeness of the created metamodels according to the relevant statistical criteria and indicators.

After the necessary experimental measurements are performed and computational models are prepared, it is important to implement a productive strategy for the optimization process in the reduced search space. At this stage, a stochastic metaheuristic hybrid particle swarm global optimization algorithm PSO with evolutionary swarm composition formation, which is a low-level hybridization with the genetic algorithm GA, was used to find the extremum of the target function. The hybrid has proven its effectiveness in solving many practical problems, for example, in [31–33]. To reconstruct the profiles, the target function was compiled on the basis of the least squares method, which was minimized by comparing the simulated ECP signal with its experimental measured value when varying the EC and MP profiles:

$$\begin{aligned} F(\boldsymbol{\sigma},\boldsymbol{\mu},f\ldots)=&\left(\mathrm{Re}(e_{mes})-\mathrm{Re}(e_{metamod})\right)^2+\\ &+\left(\mathrm{Im}(e_{mes})-\mathrm{Im}(e_{metamod})\right)^2\to\min, \end{aligned} \qquad (8)$$

where $\boldsymbol{\sigma}$, $\boldsymbol{\mu}$ are the corresponding vectors of electrophysical properties of the TO that determine the desired profiles; $e_{metamod}$ is the EMF probe was calculated by the surrogate model.

The final stage of the framework involves projecting the found profiles of the electrophysical parameters of the TO from the reduced space to the original one. The inverse transformation is performed by an iterative process [31], which embodies the corresponding reproduction and is possible when using the Gaussian kernel function.

Numerical experiments. Let us demonstrate the main stages of the proposed methodology through numerical experiments. These experiments do not require any measurements of the ECP. Therefore, the first stage will be implemented with synthesized data, which will be obtained later at the stage of creating a surrogate model.

At the second stage to apply the electrodynamic model, we consider its parameters to be set: discretized profiles of the EC $\sigma_i(z)$ and MP $\mu_i(z)$, i = 1, ... , L, where L = 60; f = 2 kHz, r_1 = 32 mm, r_2 = 50 mm, z_1 = 1 mm, z_2 = 18 mm, I = 1 A, W = 100, r = 25 mm, z = 1 mm, w_{mes} = 50.

Since the modeling was limited to only two main factors, a combination of LP$_\tau$-sequences ξ_1, ξ_6 was used to implement a homogeneous quasi-design of the experiment. The creation of discretized profiles based on this design will be presented later. The number of samples was N = 2820. The homogeneity of DOE in a unit square is demonstrated in Fig. 2,*b* a bivariate histogram and Voronoi diagram [20, 21]. Only a limited number of points, namely 256, are shown for the convenience of visualizing the DOE homogeneity in Fig. 2,*b*. The quality of this design is estimated by the numerical index WSCD = $3.157\cdot10^{-7}$ [20].

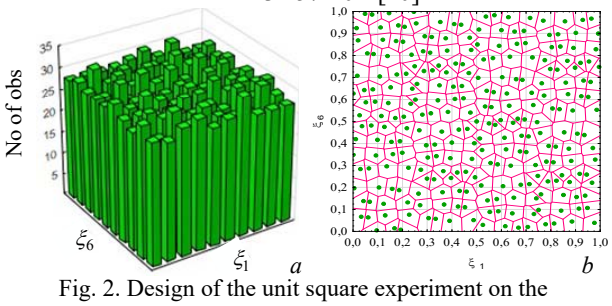

Fig. 2. Design of the unit square experiment on the LP$_\tau$-quasi Sobol's sequences ξ_1, ξ_6:
a – bivariate histogram; *b* – Voronoi diagram

Later on, the scaling was used to move to the dimensions of real space. Let us dwell on this in more detail. The zone of penetration of the electromagnetic field inside the TO is determined by the parameter $D = 3\cdot10^{-4}$ m. Before the microstructure changes, the TO is characterized by constant values of EC σ_{deep} and MP μ_{deep}. When the TO is exposed to any of the electrophysical factors (temperature, deformation, etc.), the values of the EC and MP change to the maximum on the surface to σ_{surf} and μ_{surf}, remaining unchanged at some depth of the zone. Due to the influence of uncontrollable physical factors, we assume that the values of σ_{surf} and μ_{surf} can vary within some apriori defined limits, for example, within ±15 %. In this case, the profiles are characterized by the values of EC $\sigma_{deep} = 2\cdot10^6$ S/m, $\sigma_{surf} = 9.2\cdot10^6$ S/m and MP – μ_{deep} = 10, μ_{surf} = 29.78, within which they vary in accordance with the established patterns determined previously.

Table 1 shows the numerical values of the electrophysical properties μ_{surf} and σ_{surf} on the surface of the TO at the DOE points (Fig. 2,*b*) projected by scaling into the real factor space. Then, taking into account the specified limits, the ranges of change in the EC parameters on the surface of the TO will be $7.82\cdot10^6 \le \sigma_{surf} \le 10.1\cdot10^6$ S/m, and the MP will be $24.531 \le \mu_{surf} \le 35.028$, with σ_{deep} and μ_{deep} being unchanged at the depth of the field penetration zone for any profiles.

During the modeling, we consider the laws of distribution of the electrophysical properties of the TO to be known and previously determined [21], namely, the EC is «exponential», the MP is «gaussian». Then, within the specified boundary limits of changes in electrophysical properties in the real design space (Table 1), we calculated the distributions of EC and MP for all DOE samples with discretization into a specified number of conditional As a result, we obtained a data set in the full factor space of size $N\times2L$, i.e., the dimension of the factor space is 120, which is quite significant layers.

Table 1

Scaled design of the experiment

Parameters	Design of experiment samples							
	1	2	3	…	2817	2818	2819	2820
$\sigma_{surf}\times10^6$, S/m	9.2	9.89	8.51	…	7.952756	8.642756	1.002276	9.677756
μ_{surf}	29.78	27.155	32.405	…	29.813	27.188	32.438	25.876

Some of the obtained profiles are shown in Fig. 3, and their numerical values are given in Table 2 to present the laws of distribution of the EC and MP, which are inherent in changes in the field penetration zone.

The third stage involves the calculations of the model value of the EMF e_{mod} of the probe, which are also included in Table 2, at the points of the formed design using a high-cost electrodynamic model [7].

At the fourth stage, the Kernel PCA method was used to reduce the dimensionality of the search space. To implement it, a number of mathematical transformations were performed: first, the transition from the original feature space to the auxiliary high-dimensional one was performed by projecting the DOE from dimension D to dimension N using a Gaussian kernel [31]. As a result, the kernel similarity matrix $\boldsymbol{K}$ of dimension $N\times N$ is obtained. Secondly, we apply the centering operation [31] to the kernel matrix and obtain the Gram matrix.

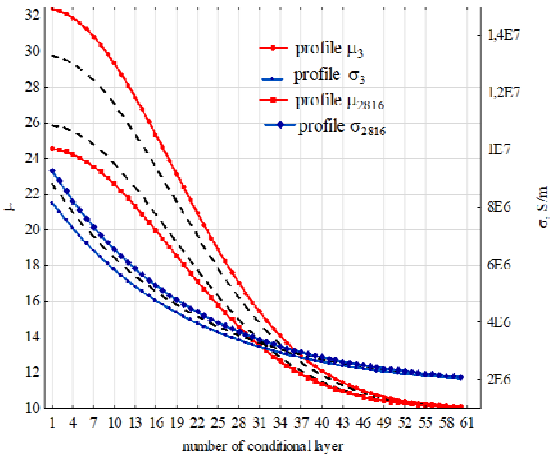

Fig. 3. Some profiles of MP and EC in the field penetration zone in the TO

Table 2

Array of initial data in the full factor space 2820×120

Profiles	Parameter	Numbers of conditional layers					ECP signal	
		1	2	…	59	60	Re(e_{mod})	Im(e_{mod})
1	μ	29.750	29.663	…	10.115	10.096	–0.737	–1.427
	σ, S/m	8834221	8486281	…	2092548	2073403		
2	μ	27.129	27.054	…	10.0994	10.083	–0.746	–1.389
	σ, S/m	9490569	9110618	…	2128662	2107756		
…	…	…	…	…	…	…	…	…
2818	μ	27.163	27.087	…	10.0997	10.083	–0.742	–1.427
	σ, S/m	8304154	7982065	…	2063382	2045659		
2819	μ	32.405	32.306	…	10.130	10.109	–0.734	–1.419
	σ, S/m	9616850	9230741	…	2135611	2114366		
2820	μ	25.852	25.782	…	10.092	10.077	–0.748	–1.386
	σ, S/m	9288676	8918572		2117553	2097189		

Third, we performed a standard linear PCA on the Gram matrix data, which assumes a singular value decomposition of the SVD [6]. Eventually, we have matrices of eigenvectors and a diagonal matrix containing eigenvalues, or rather singular numbers whose squares are eigenvalues. The ranking of the eigenvalues in the direction of reduction $\lambda_1 \geq \lambda_2 \geq ... \geq \lambda_N \geq 0$, which determines the eigenvectors for the reduced space, is shown in Fig. 4.

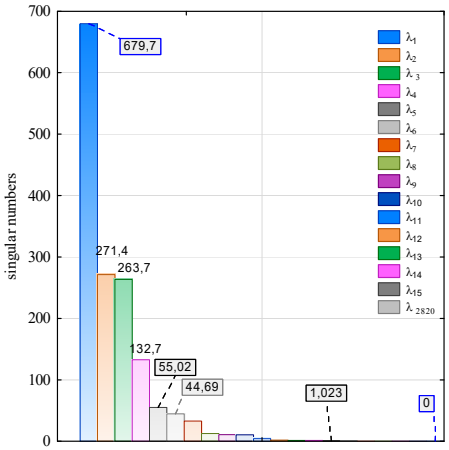

Fig. 4. Diagram of eigenvalues of the matrix

We select the first M eigenvectors under the condition $M<D$. Consequently, the first 15 eigenvectors whose singular values are greater than one, have been chosen. The reduced eigenvector matrix of dimension $N\times M$ is obtained, the elements of which g_{ij} are shown in Table 3.

Thus, the dimensionality reduction is carried out by projecting the original data onto the 15 selected principal components.

Table 3

Reduced design matrix for creating a metamodel with dimension 2820×15

Samples	Elements of a reduced plan matrix				
	$g^{(1)}$	$g^{(2)}$	…	$g^{(14)}$	$g^{(15)}$
1	–0.0128	8.0135	…	0.000046289	0.000075681
2	–14.5184	0.8005	…	–0.0091929	–0.0018594
3	14.5202	–0.0864	…	0.0088841	0.0016829
4	15.1605	–4.2985	…	0.0308	0.0079691
5	–8.9933	5.429	…	0.0348	–0.0182
…	…	…	…	…	…
2817	17.1196	–7.4162	…	–0.0212	–0.0326
2818	12.6383	2.9075	…	–0.0146	0.003627
2819	–15.7642	–2.18	…	–0.0274	–0.00028853
2820	–10.3193	3.5479	…	0.0234	0.0203

The next step is to create neural network surrogate models [18, 19] based on deep ANNs, for which the outputs of each of the two networks are the real and imaginary parts of the probe signal, respectively, and the inputs are samples of the reduced eigenvector matrix (Table 3). The division of samples was performed according to the ratio: 80 % for NN training, 9.5 % for testing and cross-validation. The data from one percent of the samples were not used in training, but later some of them were used as synthesized data to verify the reliability of the solution to the inverse profile reconstruction problem.

Thus, two neural networks were obtained, each of which is characterized by an architecture of four hidden layers Re-MLP-14-9-9-7-1 and Im-MLP-15-13-10-9-1. In each hidden layer, the activation function of the hyperbolic tangent was used, and in the output layer, the linear one. The validity of the obtained metamodels was assessed visually by histograms of residuals, normal probability plots of residuals, scatter plots, and box plots. In addition, their numerical validity is confirmed by the small values of the error $MAPE_{metamod}$, % (Mean Absolute Percentage Error). Figure 5 shows the values of these errors for both metamodels separately for the training, cross-validation, and test samples.

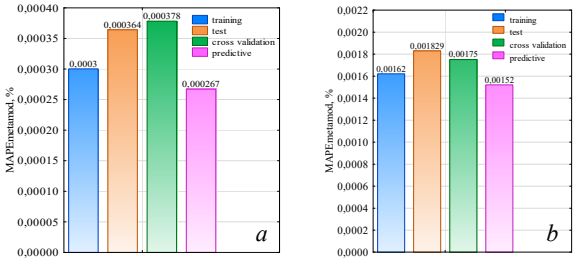

Fig. 5. Statistical assessment of the quality of metamodels by MAPE indicators:
a) Re-MLP-14-9-9-7-1; *b*) Im-MLP-15-13-10-9-1

The final step of this stage is to check the adequacy and informativeness of the created metamodels according to Fisher's criterion at a significance level of 5 % [19, 32]. Both of the created metamodels are adequate, since the estimated model values of the Fisher's criterion for them significantly exceed its critical value. Thus, the Re-MLP-14-9-9-7-1 metamodel has a Fisher's index value of $F^{total}_{15;2804} = 1.5\cdot 10^9$, and the critical value of this criterion with a significance level of α = 5 % and the number of degrees of freedom v_R = 2804, v_D = 15 is $F^{table}_{0.05;15;2804} = 1.67$, which complies with the adequacy terms. For the metamodel Im-MLP-15-

13-10-9-1, the condition of adequacy according to this criterion is also met, since $F^{total}_{15;2804} = 2.39 \cdot 10^8$. The coefficient of determination for both metamodels is $R^2 = 0.98$, which indicates their high informativeness.

Consequently, computational models can be involved in the optimization process in a reduced search space, due to which the next stage is implemented. To verify the reliability of the solution to the inverse problem of profile reconstruction, the synthesized data reserved at the stage of building the metamodel were used. Table 4 shows three examples for testing.

Due to their properties, it is advisable to use metaheuristic algorithms for optimization [33–36]. Therefore, the inverse problem for the three test samples was solved by means of a stochastic metaheuristic hybrid global optimization algorithm [6, 30]. The target function is minimized by comparing the theoretical and synthesized signals of the ECP (Table 4). In other words, a series of starts of the optimization algorithm was carried out and solution vectors were obtained in the reduced space, the results of which were averaged. In essence, the application of the multistart technique improved the accuracy of the solution.

Table 4

Test samples for verification of the procedure for determining the profiles of electrophysical property of TO

Test samples		Conditional layers					ECP signals	
		1	2	…	59	60	Re(e_{mes})	Im(e_{mes})
1	μ_{test}	26.446	26.373	…	10.095	10.080	–0.748	–0.7482
	σ_{test}, S/m	9529687	9147829	…	2130815	2109804		
2	μ_{test}	25.791	25.721	…	10.092	10.077	–0.751	–0.752
	σ_{test}, S/m	10021950	9616082	…	2157900	2135568		
3	μ_{test}	34.964	34.854	…	10.145	10.122	–0.726	–0.726
	σ_{test}, S/m	9037426	8679576	…	2103729	2084039		

The final stage is the projection of the found profiles of the electrophysical properties of the OC into the original space using the iterative inverse transformation of Kernel PCA. Thus, we have an actual solution to the inverse problem of finding electrophysical properties in the original space. The accuracy of this solution is assessed by the values of the absolute error in determining the components of the vectors of the desired parameters, given the known solution vectors μtest and σ_{test} (Table 4). Table 5 shows the values of these errors for the EC and MP profiles for each conditional layer, respectively, for three test cases.

Table 5

Values of absolute errors of profile reconstruction

Test samples		Conditional layers					
		1	2	3	…	59	60
1	$\Delta_\mu \cdot 10^{-3}$	–9.09	–9.05	–8.98	…	–0.0543	–0.0449
	Δ_σ	–2789	–2653	–2524	…	–153.47	–145.98
2	$\Delta_\mu \cdot 10^{-3}$	–6.559	–6.53	–6.482	…	–0.0379	–0.0312
	Δ_σ	–1938	–1844	–1754	…	–106.79	–101.59
3	$\Delta_\mu \cdot 10^{-3}$	–11.45	–11.4	–11.31	…	–0.0662	–0.0546
	Δ_σ	–3441	–3273	–3113	…	–189.295	–180.055

Figure 6 contains a graphical representation of the relative errors and, additionally, values of the error MAPE, % reconstruction of each of the corresponding profiles.

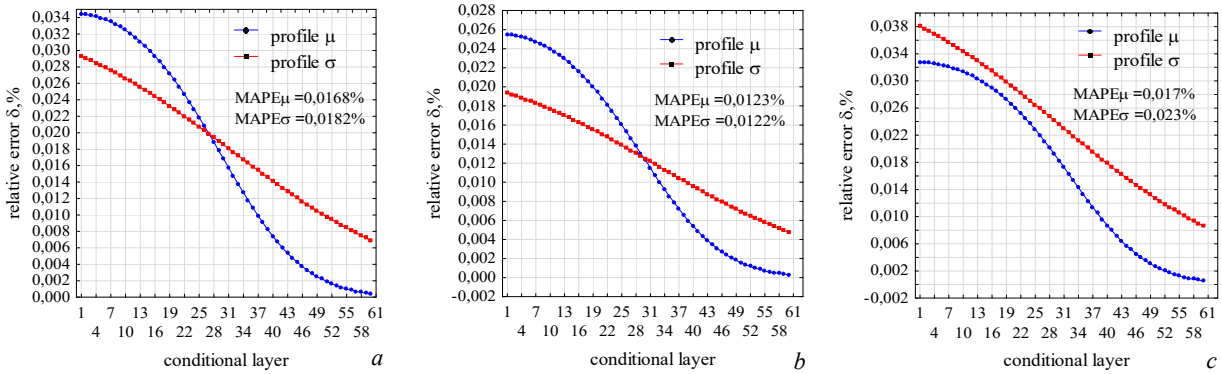

Fig. 6. Graphs of relative error distributions for EC and MP profiles: *a* – test 1; *b* – test 2; *c* – test 3

Discussions and conclusions. The most interesting result of the numerical experiments is the reduction of the search space by more than 85 %, which allowed us to move from the dimension of the primary space of 120 to the reduced one with dimension 15. It was possible due to nonlinear transformations using the Kernel PCA and the Gaussian kernel function with the analysis of the eigenvalues of the resulting Gram matrix and the limitation on the number of principal components of the linear PCA when its eigenvalues are less than one. This allowed for much more cost-effective implementation of surrogate models and optimization in a significantly reduced search space. The results confirmed the validity of such a significant reduction in space without a substantial loss of information.

Another indicator proving the effectiveness of the proposed method is the high accuracy of the created surrogate models, which is estimated by the errors $MAPE_{metamod}$ and is $0.318 \cdot 10^{-3}$ and $1.65 \cdot 10^{-3}$ %, respectively. This accuracy of the reduced-dimensional metamodels was achieved through the use of homogeneous computer DOE and deep learning networks. The adequacy and informativeness of the constructed surrogate models have been proved by numerical indicators.

Verification of the method for reconstructing the electrophysical properties of the testing object was carried

out on synthetically generated data (test samples) that are known in advance. As a result of the study, it was found that the errors MAPE of profile reconstruction for the test cases in comparison with theoretical solutions do not exceed 0.05 %, i.e., much better than the solution of the problem in the full-factor and PCA spaces, where the maximum errors reached 5.53 % and 0.96 %, respectively. In addition, it should be noted that this error contains a number of essential components: first, the error of reduction of the primary space, second, the error of approximation using surrogate models based on neural networks, third, the error of solving the inverse problem by the global optimization algorithm, and the error of projecting the found profiles of the electrophysical properties of the TO into the primary space.

Thus, the proposed computer-economical method for determining the electrophysical properties of planar metal objects by means of surrogate optimization with the accumulation of additional apriori knowledge about them in neural network metamodels with nonlinearly reduced dimensionality has demonstrated its effectiveness and ability to sufficiently accurately solve the problem of simultaneous determination of the profiles of electrical conductivity and magnetic permeability in eddy current measurements. It can be used to assess the quality of various technological processes, or the effects of uncontrolled exposure to aggressive media on the TO during their monitoring.

Conflict of interest. The authors declare that they have no conflicts of interest.

REFERENCES

1. Sabbagh H.A., Murphy R.K., Sabbagh E.H., Aldrin J.C., Knopp J.S. *Computational Electromagnetics and Model-Based Inversion*. Springer New York, 2013. 448 p. doi: https://doi.org/10.1007/978-1-4419-8429-6.

2. Liu G.R., Han X. *Computational Inverse Techniques in Nondestructive Evaluation*. CRC Press, 2003. 592 p. doi: https://doi.org/10.1201/9780203494486.

3. Di Barba P. *Multiobjective Shape Design in Electricity and Magnetism*. Springer, 2010. 313 p. doi: https://doi.org/10.1007/978-90-481-3080-1.

4. Argoul P. *Overview of Inverse Problems*. DEA. Parameter Identification in Civil Engineering, Ecole Nationale des Ponts et chaussées, 2012. 13 p.

5. Xia Z., Huang R., Chen Z., Yu K., Zhang Z., Salas-Avila J.R., Yin W. Eddy Current Measurement for Planar Structures. *Sensors*, 2022, vol. 22, no. 22, art. no. 8695. doi: https://doi.org/10.3390/s22228695.

6. Halchenko V.Y., Trembovetska R., Tychkov V., Tychkova N. Surrogate methods for determining profiles of material properties of planar test objects with accumulation of apriori information about them. *Archives of Electrical Engineering*, 2024, pp. 183-200. doi: https://doi.org/10.24425/aee.2024.148864.

7. Lu M. *Forward and inverse analysis for non-destructive testing based on electromagnetic computation methods.* PhD Thesis, The University of Manchester, UK, 2018. 224 p.

8. Campbell S.D., Sell D., Jenkins R.P., Whiting E.B., Fan J.A., Werner D.H. Review of numerical optimization techniques for meta-device design [Invited]. *Optical Materials Express*, 2019, vol. 9, no. 4, pp. 1842-1863. doi: https://doi.org/10.1364/OME.9.001842.

9. Tesfalem H., Hampton J., Fletcher A.D., Brown M., Peyton A.J. Electrical Resistivity Reconstruction of Graphite Moderator Bricks From Multi-Frequency Measurements and Artificial Neural Networks. *IEEE Sensors Journal*, 2021, vol. 21, no. 15, pp. 17005-17016. doi: https://doi.org/10.1109/JSEN.2021.3080127.

10. Hampton J., Fletcher A., Tesfalem H., Peyton A., Brown M. A comparison of non-linear optimisation algorithms for recovering the conductivity depth profile of an electrically conductive block using eddy current inspection. *NDT & E International*, 2022, vol. 125, art. no. 102571. doi: https://doi.org/10.1016/j.ndteint.2021.102571.

11. Tesfalem H., Peyton A.J., Fletcher A.D., Brown M., Chapman B. Conductivity Profiling of Graphite Moderator Bricks From Multifrequency Eddy Current Measurements. *IEEE Sensors Journal*, 2020, vol. 20, no. 9, pp. 4840-4849. doi: https://doi.org/10.1109/JSEN.2020.2965201.

12. Xu J., Wu J., Xin W., Ge Z. Measuring Ultrathin Metallic Coating Properties Using Swept-Frequency Eddy-Current Technique. *IEEE Transactions on Instrumentation and Measurement*, 2020, vol. 69, no. 8, pp. 5772-5781. doi: https://doi.org/10.1109/TIM.2020.2966359.

13. Xu J., Wu J., Xin W., Ge Z. Fast measurement of the coating thickness and conductivity using eddy currents and plane wave approximation. *IEEE Sensors Journal*, 2021, vol. 21, no. 1, pp. 306-314. doi: https://doi.org/10.1109/JSEN.2020.3014677.

14. Huang P., Zhao J., Li Z., Pu H., Ding Y., Xu L., Xie Y. Decoupling Conductivity and Permeability Using Sweep-Frequency Eddy Current Method. *IEEE Transactions on Instrumentation and Measurement*, 2023, vol. 72, pp. 1-11. doi: https://doi.org/10.1109/TIM.2023.3242017.

15. Hampton J., Tesfalem H., Fletcher A., Peyton A., Brown M. Reconstructing the conductivity profile of a graphite block using inductance spectroscopy with data-driven techniques. *Insight - Non-Destructive Testing and Condition Monitoring*, 2021, vol. 63, no. 2, pp. 82-87. doi: https://doi.org/10.1784/insi.2021.63.2.82.

16. Yi Q., Tian G.Y., Malekmohammadi H., Laureti S., Ricci M., Gao S. Inverse reconstruction of fibre orientation in multilayer CFRP using forward FEM and eddy current pulsed thermography. *NDT & E International*, 2021, vol. 122, art. no. 102474. doi: https://doi.org/10.1016/j.ndteint.2021.102474.

17. Arridge S., Maass P., Öktem O., Schönlieb C.-B. Solving inverse problems using data-driven models. *Acta Numerica*, 2019, vol. 28, pp. 1-174. doi: https://doi.org/10.1017/S0962492919000059.

18. Halchenko V.Ya., Trembovetska R.V., Tychkov V.V., Sapogov M.M., Gromaszek K., Smailova S., Luganskaya S. Additive neural network approximation of multidimensional response surfaces for surrogate synthesis of eddy-current probes. *Przegląd Elektrotechniczny*. 2021, no. 9, pp. 46-49. doi: https://doi.org/10.15199/48.2021.09.10.

19. Halchenko V.Y., Trembovetska R.V., Tychkov V.V. Development of excitation structure rbf-metamodels of moving concentric eddy current probe. *Electrical Engineering & Electromechanics*, 2019, no. 2, pp. 28-38. doi: https://doi.org/10.20998/2074-272X.2019.2.05.

20. Trembovetska R., Halchenko V., Bazilo C. Inverse Multi-parameter Identification of Plane Objects Electrophysical Parameters Profiles by Eddy-Current Method. *Lecture Notes in Networks and Systems*, 2023, vol. 536 LNNS, pp. 202-212. doi: https://doi.org/10.1007/978-3-031-20141-7_19.

21. Uzal E. *Theory of eddy current inspection of layered metals*. PhD Dissertation. Iowa State University, 1992. 190 p. doi: https://doi.org/10.31274/rtd-180813-9635.

22. Bowler N. *Eddy-current nondestructive evaluation*. Springer, New York. 2019, 217 p. doi: https://doi.org/10.1007/978-1-4939-9629-2.

23. Lei Y.-Z. General series expression of eddy-current impedance for coil placed above multi-layer plate conductor. *Chinese Physics B*, 2018, vol. 27, no. 6, art. no. 060308. doi: https://doi.org/10.1088/1674-1056/27/6/060308.

24. Zhang J., Yuan M., Xu Z., Kim H.-J., Song S.-J. Analytical approaches to eddy current nondestructive evaluation for stratified conductive structures. *Journal of Mechanical Science and Technology*, 2015, vol. 29, no. 10, pp. 4159-4165. doi: https://doi.org/10.1007/s12206-015-0910-7.

25. Theodoulidis T.P., Kriezis E.E. *Eddy current canonical problems (with applications to nondestructive evaluation*). Tech Science Press. 2006, 259 p.
26. Halchenko V., Trembovetska R., Bazilo C., Tychkova N. Computer simulation of the process of profiles measuring of objects electrophysical parameters by surface eddy current probes. *Lecture Notes on Data Engineering and Communications Technologies*, 2023, vol. 178, pp. 411-424. doi: https://doi.org/10.1007/978-3-031-35467-0_25.
27. Dodd C.V., Deeds W.E. *Calculation of magnetic fields from time-varying currents in the presence of conductors*. Technical Report no. ORNL-TM-4958, Oak Ridge National Laboratory, Tennessee, United States, 1975. 35 p.doi: https://doi.org/10.2172/4178400.
28. Raschka S. Mirjalili, V. *Python Machine Learning: Machine Learning and Deep Learning with Python, scikit-learn, and TensorFlow 2, 3rd Ed.* Packt Publ., 2019. 772 p.
29. Schölkopf B., Smola A.J. (2001). *Learning with Kernels: Support Vector Machines, Regularization, Optimization, and Beyond*. The MIT Press, 2001. 626 p. doi: https://doi.org/10.7551/mitpress/4175.001.0001.
30. Halchenko V.Y., Trembovetska R.V., Tychkov V.V. Synthesis of eddy current probes with volumetric structure of the excitation system, implementing homogeneous sensitivity in the testing zone. *Technical Electrodynamics*, 2021, no. 3, pp. 10-18. (Ukr). doi: https://doi.org/10.15407/techned2021.03.010.
31. Wang Q. *Kernel principal component analysis and its applications in face recognition and active shape models*. 2012, doi: https://doi.org/10.48550/arXiv.1207.3538.
32. Montgomery D.C. *Design and Analysis of Experiments. 10th ed.* John Wiley and Sons, 2020. 688 p.
33. Kuznetsov B., Nikitina T., Bovdui I., Voloshko O., Chunikhin K., Dobrodeyev P. Electromagnetic Shielding of Two-Circuit Overhead Power Lines Magnetic Field. *Problems of the Regional Energetics*, 2023, vol. 4, no. 60, pp. 14-29. doi: https://doi.org/10.52254/1857-0070.2023.4-60.02.
34. Kuznetsov B.I., Nikitina T.B., Bovdui I.V., Voloshko O.V., Kolomiets V.V., Kobylianskyi B.B. Optimization of spatial arrangement of magnetic field sensors of closed loop system of overhead power lines magnetic field active silencing. *Electrical Engineering & Electromechanics*, 2023, no. 4, pp. 26-34. doi: https://doi.org/10.20998/2074-272X.2023.4.04.
35. Koshevoy N.D., Muratov V.V., Kirichenko A.L., Borisenko S.A. Application of the "jumping frogs" algorithm for research and optimization of the technological process. *Radio Electronics, Computer Science, Control*, 2021, no. 1, pp. 57-65. doi: https://doi.org/10.15588/1607-3274-2021-1-6.
36. Koshevoy N.D., Kostenko E.M., Muratov V.V. Application of the fish search method for optimization plans of the full factor experiment. *Radio Electronics, Computer Science, Control*, 2020, no. 2, pp. 44-50. doi: https://doi.org/10.15588/1607-3274-2020-2-5.

Received 04.06.2024
Accepted 21.08.2024
Published 02.01.2025

V.Ya. Halchenko[1], *Doctor of Technical Science, Professor,*
R.V. Trembovetska[1], *Doctor of Technical Science, Associate Professor,*
V.V. Tychkov[1], *Candidate of Technical Science, Associate Professor,*
[1] Cherkasy State Technological University,
460, Blvd. Shevchenka, Cherkasy, 18006, Ukraine,
e-mail: v.halchenko@chdtu.edu.ua; r.trembovetska@chdtu.edu.ua; v.tychkov@chdtu.edu.ua (Corresponding Author)

How to cite this article:
Halchenko V.Ya., Trembovetska R.V., Tychkov V.V. Computer-economical optimization method for solving inverse problems of determining electrophysical properties of objects in eddy current structroscopy. *Electrical Engineering & Electromechanics*, 2025, no. 1, pp. 3-11. doi: https://doi.org/10.20998/2074-272X.2025.1.01